












Research Article

Chemical Characterization, Antioxidant, and Antihyperglycemic Capacity of Ferulated Arabinoxylan Extracted from “Chicha de Jora” Bagasse: An Ancestral Fermented Beverage from *Zea mays* L.

Juan Jharol Segovia-Huarcaya ¹, Lilian Silvana Valentin-Soto ¹,
Oscar Herrera-Calderon ¹, César Máximo Fuertes-Ruitón ²,
Josefa Bertha Pari-Olarde ³, Eddie Loyola-Gonzales ⁴,
José Santiago Almeida-Galindo ⁵, José Francisco Kong-Chirinos ⁶,
Elizabeth Julia Melgar-Merino ⁷, Mohammed Merae Alshahrani ⁸,
and Shafi Mahmud ⁹

¹Department of Pharmacology, Bromatology and Toxicology, Faculty of Pharmacy and Biochemistry, Universidad Nacional Mayor de San Marcos, Jr. Puno 1002, Lima 1002, Peru

²Institute for Research in Pharmaceutical Sciences and Natural Resources, Faculty of Pharmacy and Biochemistry, Universidad Nacional Mayor de San Marcos, Jr. Puno 1002, Lima 15001, Peru

³Department of Pharmaceutical Chemistry, Faculty of Pharmacy and Biochemistry, Universidad Nacional San Luis Gonzaga, Ica, Peru

⁴Department of Pharmaceutical Sciences, Faculty of Pharmacy and Biochemistry, Universidad Nacional San Luis Gonzaga, Ica, Peru

⁵Department of Surgical Clinical Sciences, Faculty of Human Medicine, Universidad Nacional San Luis Gonzaga, Ica, Peru

⁶Department of Basic Sciences, Faculty of Human Medicine, Universidad Nacional San Luis Gonzaga, Ica, Peru

⁷Department of Chemistry Sciences, Faculty of Pharmacy and Biochemistry, Universidad Nacional San Luis Gonzaga, Ica, Peru

⁸Department of Clinical Laboratory Sciences, Faculty of Applied Medical Sciences, Najran University, Najran 61441, Saudi Arabia

⁹Division of Genome Sciences and Cancer, The John Curtin School of Medical Research, and The Shine-Dalgarno Centre for RNA Innovation, The Australian National University, Canberra 2601, Australian Capital Territory, Australia

Correspondence should be addressed to Oscar Herrera-Calderon; oherreraca@unmsm.edu.pe

Received 28 April 2022; Revised 18 May 2022; Accepted 23 May 2022; Published 10 June 2022

Academic Editor: Imran Ali

Copyright © 2022 Juan Jharol Segovia-Huarcaya et al. This is an open access article distributed under the Creative Commons Attribution License, which permits unrestricted use, distribution, and reproduction in any medium, provided the original work is properly cited.

Bagasse is a byproduct generated during the process of making the traditional Andean drink named “chicha de jora” in Peru, which is a potential source for the extraction of ferulated arabinoxylan (FAX). The aim of this study was to extract and characterize the FAX from bagasse and determine its antioxidant and antihyperglycemic capacity in vitro. As a result, FAX of molecular weight ≥ 3.5 kDa presented moisture content, pH, total ash, proteins, and total phenolic content with values of 8.00%, 5.81, 2.68%, 3.78%, and 5.72 mg EAG/g, respectively. Thin-layer chromatography identified the monosaccharides L-arabinose and D-xylose. HPLC-MS/MS analysis of FAX confirmed the presence of methyl-pentofuranosides or methyl-pentopyranosides. The FT-IR spectrum presented characteristic bands of FAX. The FAX showed antioxidant capacity determined by the DPPH assay ($IC_{50} = 6.59$ mg/mL and $TEAC = 7.7844$ μ mol/g sample), ABTS ($IC_{50} = 6.50$ mg/mL and $TEAC 35.34$ μ mol/g sample), and FRAP (14.08 μ mol AA/g and 36.63 μ mol $FeSO_4$ /g). On the other hand, FAX showed glucose adsorption capacity, inhibition of glucose diffusion, and inhibition of the enzyme α -amylase ($IC_{50} = 4.73$ mg/mL). The results showed that the FAX extracted from the bagasse generated during the production of the “chicha de jora” has in vitro antioxidant and antihyperglycemic capacity.

1. Introduction

Chicha de jora (CJ) is a traditional Peruvian beverage with low alcohol content (1–3%) similar to beer, that is produced by fermentation of the germinated corn (*Zea mays*). This beverage is produced with indigenous technology in places called “chicherias” [1], and the general steps for its preparation are shown in Figure 1. Its preparation generates a byproduct called bagasse which has mainly residues of corn husk constituting polysaccharides such as cellulose, hemicellulose, and lignin. The most representative hemicellulose of the bagasse is the ferulated arabinoxylan (FAX) which has potential application in the food, pharmaceutical, and cosmetics industry [2]. FAX chemically consists in a linear chain of D-xyloses linked by β -(1 \rightarrow 4) glycosidic bonds, with substituents of D-arabinose by α -(1 \rightarrow 3) or α -(1 \rightarrow 2) glycosidic linkages, or both; some residues of D-arabinose have substituents of ferulic acid esterified in C-5 [3].

FAX has biological properties reported in the scientific literature, such as antioxidant, antidiabetic, anticoagulant, anti-inflammatory, antimicrobial, immunoregulatory, and anticancer capacity [4]. Si et al. [5] extracted FAX from corn bran and evidenced a proportional relation between the presence of phenolic compounds linked to the polysaccharide and its antioxidant capacity. The polysaccharide is mainly esterified with ferulic acid but has been reported the presence in low proportion of other phenolic compounds such as p-coumaric and cinnamic acid [6]. Other factors including molecular weight, degree of polymerization, and ratio of arabinose and xylose (Ara/Xil) of the polysaccharide are responsible for its antioxidant capacity [7]. Additionally, Kamboj and Rana [8] showed that the antioxidant potential of the FAX isolated from corn bran is higher than polysaccharides such as guar gum, sulfated guar gum, and xanthan oligosaccharide.

The FAX has the ability to inhibit the enzymatic activity of the sucrase and maltase in vitro, and it can also inhibit transporters of glucose-independent sodium 2 (GLUT2) in oocytes [9]. Huang et al. [10] investigated the antidiabetic capacity in vivo of ferulated oligosaccharides from corn bran in male rats with diabetes induced by streptozotocin (STZ), concluding that a dose of 600 mg/kg/day reduces significantly glucose, insulin, and LDL levels and increases HDL levels. Similarly, Nie et al. [11] reported that the FAX extracted from *Plantago asiatica* improves the metabolism of carbohydrates, lipids, and amino acids in rats with diabetes induced by STZ and a high-fat diet.

However, to date, the use of this byproduct has not been considered because there is no report in the scientific literature that supports its potential benefits. In the present study, FAX from bagasse of the CJ is extracted by alkaline hydrogen peroxide. The antioxidant and antihyperglycemic capacity in vitro is also examined.

2. Materials and Methods

2.1. Materials. Bagasse of chicha de jora (traditionally called in Peru “sutuchi”) was kindly provided by Misky S. A. C. (Cusco, Peru). It was washed 4 times with tap water, dried at 400°C for 48 h, and milled to a 20-mesh particle size. Thermostable α -amylase from *Bacillus licheniformis*, L-arabinose, D-xylose, D-glucose, acarbose, glucose oxidase enzyme assay kit, and α -amylase from porcine pancreas were purchased from Sigma-Aldrich (St. Louis, MO, USA). Other chemicals were analytical grade.

2.2. Extraction of Ferulated Arabinoxylan. The sample (100 g) was deoiled with n-hexane (700 mL) under 300 rpm for 2 h at 50°C [12]. Then, 75 g was treated with thermostable α -amylase (4.5 mL of enzyme/100 g of sample). The pH was adjusted to 6.5 with 50% NaOH and then stirred between 85 and 90°C under 300 rpm for 2.5 h in H₂O (750 mL). The fiber was washed twice with hot water and once with 96% ethanol to remove maltodextrin. It was dried at 50°C for 24 h [13].

The polysaccharides were extracted based on the work of Kamboj and Rana [8]. The deoiled and destarched sample (50 g) was added to 500 mL of H₂O with 4 g of NaOH (2 mEq of alkali/gram of fiber in the medium), and it was boiled for 1 h. Once cooled, it was centrifuged at 6000 \times g for 20 min at 25°C, and the supernatant was recovered by decantation. Then, 17 mL of 30% H₂O₂ was added to the decanted fraction, and the pH was adjusted to 11.5 with 50% NaOH and stirred at room temperature for 2 h. After the pH was adjusted between 4 and 4.5 adding concentrated HCl to precipitate hemicellulose A, which was separated by centrifugation at 7100 \times g for 20 min at 25°C. Two volumes of 96% ethanol were added to the supernatant to precipitate the main FAX fraction, hemicellulose B. The FAX was allowed to settle as a white flocculent precipitate in cold, and it was removed by vacuum filtration with 96% ethanol. And then, it was dialyzed for 48 h in tap water and 48 h in distilled water on a dialysis membrane with a molecular weight cutoff (MWCO) of 3.5 kDa. The dialyzed sample was dried at 50°C for 48 h.

2.3. Physicochemical Characterization

2.3.1. Solubility. The powdered sample was dissolved using different solvents (water, methanol, ethanol, ethyl acetate, acetone, and chloroform) according to monograph <5.11> of the European Pharmacopoeia 10.0 [14]. The solubility at different temperatures was carried out according to Kong et al.'s study [15], and the sample (100 mg) was mixed with 50 mL of H₂O under 150 rpm at 25, 40, 60, 80, and 100°C until complete dissolution.

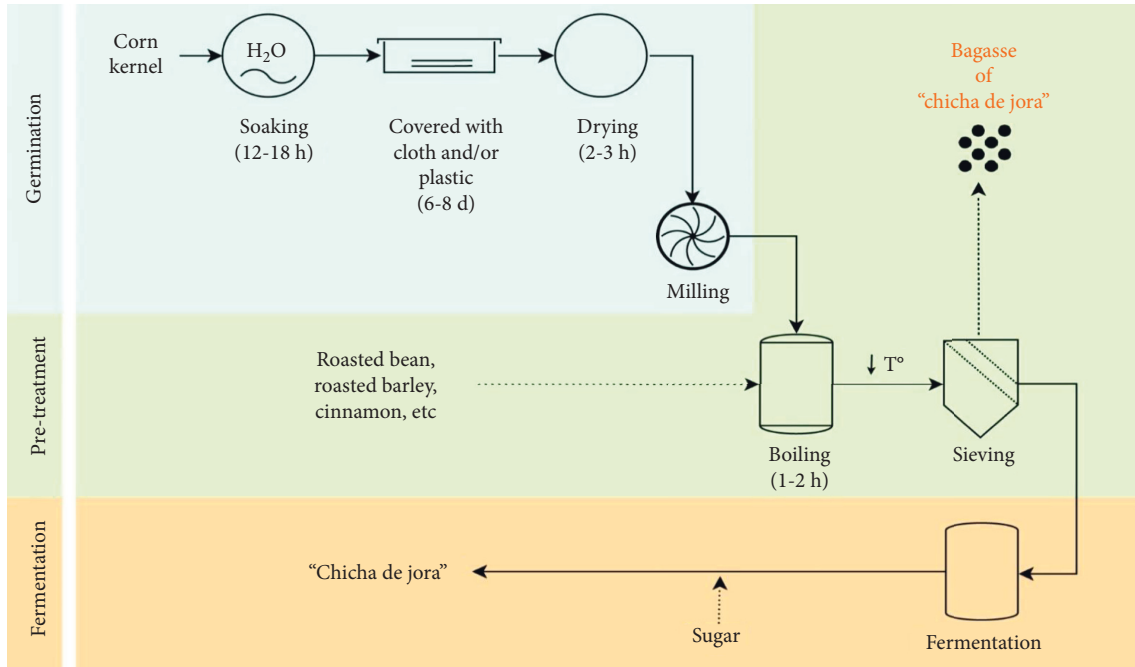


FIGURE 1: General steps for the preparation of “chicha de jora.” The bagasse is a by-product generated before the fermentation.

2.3.2. Moisture Content. The oven-drying method was used. In brief, 2 g of sample was placed on Petri dishes at 105°C for 3 h [16].

2.3.3. pH. The pH was determined in a solution of 1% (w/v) of the polysaccharide [17].

2.3.4. Total Ash. The quantification of total ash was developed using the gravimetric method [16].

2.3.5. Protein Content. The Kjeldahl method was used to quantify the protein content [16].

2.3.6. Micromeritic Analysis

(1) Angle of Repose. It was carried out following the funnel flow method indicated in the monograph <1174> of the USP 41 [18]. Initially, the tip of the funnel was kept 2 cm away from the surface. 10 g was allowed to flow freely over the funnel until a symmetrical cone was formed reaching the tip of the funnel. The height (h) and base radius (r) of the formed cone were measured and substituted into equation (1), where θ is the angle of repose.

$$\theta = \tan^{-1} \frac{h}{r}. \quad (1)$$

(2) Bulk Density and Compacted Density. Initially, 10 g of sample was carefully added in a 50 mL graduated cylinder, and the volume occupied by the sample (V_b , mL) was measured. Then, it was mechanically tapped on a flat surface,

and the volume was read after 500 taps when a constant volume (V_c , mL) was evidenced [19]. Equations (2) and (3) allowed to obtain the respective calculations.

$$\rho_b = \frac{W}{V_b}, \quad (2)$$

$$\rho_c = \frac{W}{V_c}, \quad (3)$$

where ρ_b is bulk density (g/mL), ρ_c is compacted density (g/mL), and W is the sample mass (G).

(3) Hausner Index (HI) and Carr Index (CI). The HI and the CI were calculated using the equations (4) and (5), respectively [20].

$$HI = \frac{\rho_b}{\rho_c}, \quad (4)$$

$$CI (\%) = \frac{(\rho_c - \rho_b)}{\rho_c} \times 100\%, \quad (5)$$

where ρ_b is the apparent density and ρ_c is the compacted density.

2.3.7. Viscosity. The flow time of different solutions of the sample (0.1, 0.4 and 0.8%, w/v) was measured at 30°C using an Ostwald viscometer [21]. The relative viscosity (η_{rel}) of the sample against distilled water was calculated, and formula (6) allowed the calculation of the specific viscosity (η_{sp}). The apparent intrinsic viscosity (η_{int} , dL/g) was determined using the Morris equation (7), where c is the FAX concentration:

$$\eta_{sp} = \eta_{rel} - 1, \quad (6)$$

$$\eta_{int} = \left(\frac{1}{cc}\right) \times [2 \times (\eta_{sp} - \ln \eta_{rel})] 0.5 \times 10. \quad (7)$$

2.4. Total Phenolic Content (TPC). In brief, 100 μL of sample (1%, w/v) was mixed with 150 μL of Folin–Ciocalteu reagent (1 : 10, v/v). After 5 min, 150 μL of saturated 7.5% Na_2CO_3 and 3600 μL of H_2O were added, and this mixture was incubated at room temperature in the dark for 30 min. After that, the absorbance was read at 760 nm. TPC was calculated based on a standard calibration curve of gallic acid (0.03125–0.25 mg/mL) [5].

2.5. Identification of Monosaccharides by Thin-Layer Chromatography (TLC). The sample (25 mg) was treated with 2 mL of 2 M trifluoroacetic acid (TFA) at 100°C for 2.5 h. The stationary phase was TLC Silica gel 60 F254 (Merck, Germany), and the mobile phase was chloroform, acetic acid, and water (3 : 3.5 : 0.5). After elution, it was revealed by spraying a mixture of diphenylamine (1 g) and aniline (1 mL) in acetone (100 mL), and before use was added 85% orthophosphoric acid (10 mL). The plate was dried at 100°C for 10 min.

2.6. Analysis by HPLC-MS/MS. The sample was subjected to partial hydrolysis by acid methanolysis as previously described by Eugene et al. [22]. Initially, the sample (100 μg /mL) was dried with nitrogen (N_2). After that, it was treated with 3 M methanolic HCl reagent at 65°C for 1 h and was mixed with 200 μL of acetonitrile : H_2O (9 : 1). The HPLC-MS/MS analysis used a Dionex UltiMate TM 3000 liquid chromatograph (Thermo Fisher Scientific, San Jose, USA) coupled to a Thermo QExactive™ Plus Orbitrap mass spectrometer (Thermo Fisher Scientific, Bremen, Germany) combined with electrospray negative ionization (ESI⁻). The HPLC had a Water XBridge Amide BEH chromatographic column (150 mm \times 4.6 mm \times 3.5 μm) with a mobile phase of solvent A (0.1% ammonium hydroxide, in 95% water and 5% acetonitrile) and B (0.1% ammonium hydroxide, in 95% acetonitrile and 5% water). The following conditions were used: gradient elution method: 0–2 min 95% B; 2–17 min 50% B; 17–20 min 50% B; 20–21 min 95% B; and 21–27 min 95% B; flow rate, 500 $\mu\text{L}/\text{min}$; injection of 8 μL ; and column oven at 45°C.

2.7. Mass Spectrometry Parameters. A full scan experiment combined with a fragmentation experiment (MS/MS) was performed for both modes of electrospray ionization (ESI⁺ and ⁻). The parameters of the ESI source are described as follows: spray voltage, 3.6 kV (⁻); sheath gas flow rate, 50 (arbitrary values); auxiliary gas flow rate, 10 (arbitrary values); tube lens voltage, 50 V; probe heater temperature, 400°C; capillary temperature, 300°C:

- (a) Mode (ESI⁻): full MS mode parameters: resolution 35,000 (FWHM) | ACG target: $5e^5$ | maximum IT: 100 ms | m/z range 100–1000.
- (b) Parameters of the dd-MS2 mode (data dependent acquisition experiment—DDA): resolution, 17,500 (FWHM) | ACG target: $1e^5$ | maximum IT: 50 ms | loop count 3 | isolation window m/z 1.2 | topN 3 | NCE: 15, 20, 30.
- (c) PRM (parallel reaction monitoring) parameters—MS2: resolution, 35,000 (FWHM) | ACG target: $2e^5$ | maximum IT: 100 ms | isolation window: m/z 1.2 | (N) CE = 10. The inclusion list for monitoring in the PRM method throughout the analysis: possible metabolites was according to Table 1.

2.8. Analysis by UV-Vis Spectroscopy. The sample (0.5%, w/v) was placed in quartz cuvettes to scan the spectrum between 250 and 500 nm with a Genesys™ UV/Vis spectrophotometer (Thermo Fisher Scientific, San Jose, USA).

2.9. Analysis by Infrared Spectroscopy. The dried polysaccharide was analyzed in Spectrum 100 FT-IR (PerkinElmer, Massachusetts, USA). The sample was crushed with KBr at 1 : 20 (w/w). The scan resolution was 4 cm^{-1} , between 4000 and 400 cm^{-1} .

2.10. Determination of Antioxidant Capacity In Vitro

2.10.1. DPPH• Assay. The DPPH• assay was determined by the method adopted by Marquez-Escalante and Carvajal-Millan [23] which avoids the precipitation of the sample. Initially, 50 mL of DPPH• 45 μM was prepared with methanol : water (60 : 40). Once dissolved, it was filtered through Whatman No. 1 paper and used after 1 h. Then, 400 μL of sample (0.5–10 mg/mL) was mixed with 350 μL of methanol, and 750 μL of DPPH• was added. The curve of inhibition was made with different concentrations of Trolox (0.001–0.002 mg/mL). The absorbance was measured at 515 nm after 30 min of incubation in the dark. The % inhibition of the DPPH• radical was determined by the following equation:

$$\% \text{inhibition} = \left(\frac{A_{\text{control}} - A_{\text{sample}}}{A_{\text{control}}} \right) \times 100\%, \quad (8)$$

where A_{control} is the absorbance of the control and A_{sample} is the absorbance of the sample or standard.

2.10.2. ABTS•+ Assay. Initially, 1.7 mL of 7 mM ABTS•+ (diluted to an absorbance of 0.7 ± 0.02 at 734 nm) were added to 100 μL of different concentrations of sample (0.1–10 mg/mL) and then left at rest for 7 min at room temperature, and the absorbance was measured at 734 nm. An inhibition curve of the Trolox was prepared using concentrations between 0.003 and 0.1 mg/mL [24]. The % inhibition of the ABTS•+ radical was determined using the following equation:

TABLE 1: Metabolites included in the PRM method during mass spectrometry analysis.

Metabolite	Neutral formula	ESI (-)	Theoretical (m/z)
Methyl-D-xylofuranoside			
Methyl-D-xylopyranoside	C6H12O5	[M-H] ⁻	163.06119
Methyl-D-arabinofuranoside			
Methyl-D-arabinopyranoside			
Ferulate/ferulic acid	C10H10O4	[M-H] ⁻	193.05063

$$\% \text{ inhibition} = \left(\frac{A_{\text{control}} - A_{\text{sample}}}{A_{\text{control}}} \right) \times 100\%, \quad (9)$$

where A_{control} is the absorbance of the control and A_{sample} is the absorbance of the sample or standard.

2.10.3. FRAP Assay. The FRAP reagent was recently prepared and was made by mixing acetate buffer (300 mM at pH 3.6), $\text{FeCl}_3 \cdot 6\text{H}_2\text{O}$ (20 mM), and 2,4,6-tripyridyl-S-triazine (TPTZ, 10 mM in 40 mM HCl) at ratio 10:1:1. Calibration curves were made from different concentrations of ascorbic acid (100–1000 $\mu\text{mol/L}$) and $\text{FeSO}_4 \cdot 7\text{H}_2\text{O}$ (25–1000 $\mu\text{mol/L}$). Subsequently, 50 μL of polysaccharide (40 mg/mL), 450 μL of FRAP reagent, and 1500 μL of bidistilled water were allowed to react for 10 min, and then the absorbance was determined at 593 nm [25].

2.11. Determination of In Vitro Antihyperglycemic Capacity

2.11.1. Glucose Adsorption Capacity (GAC). GAC was determined using the method of Dong et al. [26]. In brief, 0.5 g of the sample was mixed with 50 mL of different concentrations of anhydrous glucose (10–200 mmol.L^{-1}) and incubated at 37°C for 6 h. After centrifugation at 4500 $\times\text{g}$ for 20 min at 25°C, the amount of adsorbed glucose was estimated quantifying the concentration of glucose in the supernatant using the glucose oxidase enzyme kit. GAC was expressed as mmol of glucose adsorbed per gram of sample (mmol/g) and was calculated according to the following equation:

$$\text{GAC} \left(\frac{\text{mmol}}{\text{g}} \right) = \frac{C_i - C_f}{W_m}, \quad (10)$$

where C_i and C_f are the glucose content before and after of the absorption and W_m is the weight of the sample.

2.11.2. Glucose Diffusion Inhibition Capacity. The sample (2 mL) at different concentrations (1, 10, and 25 mg/mL) were placed in SnakeSkin™ Dialysis Tubing of 3.5 kD MWCO (Thermo Fisher Scientific, San Jose, USA). Then, 2 mL of glucose 0.25 M was added. The negative and positive controls were distilled water and acarbose, respectively. The dialysis tubing was sealed and then introduced in a beaker with NaCl 0.15 M (80 mL) and water (20 mL), and it was stirred at 150 rpm and 37°C. After 1 mL of the sample and controls were taken every 30 min for 180 min, glucose was quantified with a glucose oxidase enzyme kit at 505 nm. It was expressed in $\mu\text{g/mL}$ [27].

2.11.3. α -Amylase Inhibition Capacity. The test was carried out as reported previously by Inocente Camones et al. [28]. In brief, 125 μL of FAX or acarbose at different concentrations (0.1–5 mg/mL) were preincubated at 25°C for 10 min with 125 μL of α -amylase 13 U/mL (dissolved in sodium phosphate buffer 0.02 mol/L at pH 6.9). After preincubating, 125 μL of 1% soluble starch was added. Then, 250 μL of 96 mM 3,5-dinitrosalicylic acid was added. The reaction was stopped by boiling the tubes for 15 min. They were cooled at room temperature and dissolved with distilled water (3 mL) to finally read the absorbance at 540 nm. The % inhibition was calculated using the following equation:

$$\text{inhibition} (\%) = \left[1 - \frac{(A_1 - A_2)}{(A_3 - A_4)} \right] \times 100, \quad (11)$$

where A_1 , A_2 , A_3 , and A_4 are defined as the absorbance of the sample (with enzyme), absorbance of the sample blank (without enzyme), absorbance of the control with 100% activity (alone enzyme and solvent), and absorbance of the control blank with 0% activity (no enzyme), respectively.

2.12. Statistical Analysis. The data was presented as mean \pm standard deviation (SD) for three replicates. Two-way analysis of variance (ANOVA) with Turkey's post hoc test was used to make comparisons between treatments using the statistical program GraphPad Prism 6.0. Values of $p < 0.05$ were considered statistically significant.

3. Results and Discussion

3.1. Extraction of Ferulated Arabinoxylan. The yield of the chemical extraction was $19.87 \pm 4.56\%$ (see Figure 2(c)), similar to the yield previously reported for the FAX of the corn pericarp (18%) [29]. A slightly higher yield (38%) was determined by Kamboj and Rana [8]. On the other hand, Buksa et al. [30] reported a yield of 1.7% and 3.2% for the polysaccharide from wheat and rye, respectively, in both cases extracted by the aqueous method. FAX is not efficiently extracted using water as extraction solvent. Alkaline conditions allow the breaking of ester bonds and hydrogen bonds within the cell wall [31]. Alkaline solutions with H_2O_2 react rapidly with lignin to form water-soluble oxidized products of low molecular weight, which causes the rupture in the union of lignin and FAX [32].

3.2. Physicochemical Characterization

3.2.1. Solubility. FAX was soluble in water; very slightly soluble in ethyl acetate; and insoluble in methanol, ethanol, acetone, and chloroform. These results were similar to those previously reported by Höije et al. [33]. The aqueous solubility is due to the high presence of hydroxyl groups (OH^-) in the polysaccharide chain and therefore to its greater capacity to form hydrogen bonds [34]. In addition, the polysaccharide could have an amphiphilic nature in which the nonpolar region could be represented by the rings of the monosaccharide [35]. Figure 2(d)

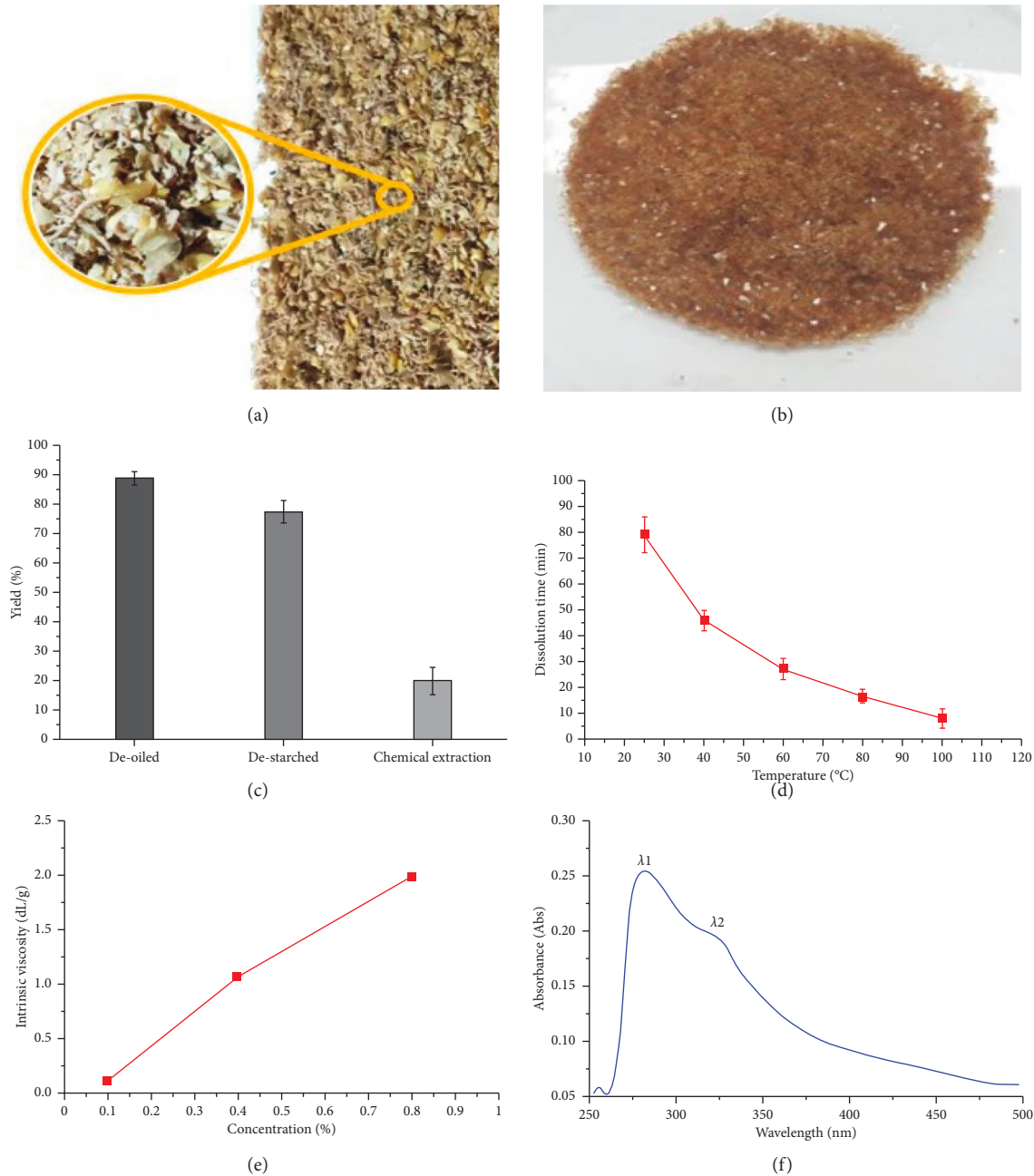


FIGURE 2: (a) Bagasse of "chicha de jora"; (b) FAX dried and milled; (c) yield of the deoiled, destarched, and chemical extraction; (d) solubility of the sample at different temperatures; (e) intrinsic viscosity at different concentration; (f) UV-vis spectrum of the sample.

shows that the highest dissolution time of 79.33 ± 7.02 min occurred at 25°C; however, at 100°C, the time was reduced to 8.00 ± 3.61 min.

3.2.2. Moisture Content. The moisture content was $8.00 \pm 1.77\%$ (see Table 2), lower than the yield of 12.1% (drying at 50°C for 96 h) for the FAX [36]. The moisture content can predict the microbial growth in the FAX sample,

and the presence of moisture accelerates decomposition and generates toxins [37].

3.2.3. pH. The pH helps us to deduce the solubility, stability, irritability, and permeability in biological membranes of a substance. Likewise, it determines the compatibility in formulations [17]. The pH was 5.81 ± 0.02 (see Table 2); however, this value is slightly more acidic than the pH

TABLE 2: Physicochemical characterization of the FAX extracted.

Physicochemical characterization	Results*
Moisture (%)	8.00 ± 1.77
pH	5.81 ± 0.02
Total ash (%)	2.68 ± 0.01
Protein (%)	3.78 ± 0.02
Angle of repose (°)	20.04 ± 0.43
Bulk density (mg/mL)	0.78 ± 0.02
Compact density (mg/mL)	0.91 ± 0.01
Hausner index	1.17 ± 0.02
Carr index (%)	14.35 ± 1.43

All the results are expressed as the mean ± S.D. ($n=3$).

(6.19 ± 0.03) of the AX from rice bran [38]. This may be due to the presence of uronic acid and a higher amount of free phenolic acids.

3.2.4. Total Ash. Table 1 shows the result of total ash (2.68 ± 0.01%). It suggests the presence of residual non-volatile inorganic substances. Generally, total ash is composed of metal oxides, carbonates, oxalates, and silicates [39]. Jacquemin et al. [40] found a high value (5.5%), and they suggested that it could be due to the presence of sodium metal derived from NaOH used during the extraction step.

3.2.5. Protein Content. The protein content was 3.78 ± 0.02% (see Table 1), similar to the value obtained for the polysaccharide from wheat (3.70%) [41]. However, the protein content in the FAX reported by Mendez-Encinas et al. [42] was 8.2%. This result indicates that proteins in the FAX form a complex that cannot be easily destabilized even under treatment with alkaline hydrogen peroxide.

3.2.6. Micromeritic Analysis. The results are summarized in the Table 1. The flow characteristic attributed to the FAX sample considering the angle of repose (20.04 ± 0.43°) was excellent. Hausner index (1.17 ± 0.02) and Carr index (14.35 ± 1.43%) indicated that the pulverized FAX presents a good flow. Our results are in line with the results of Erum et al. [43]. It should be noted that Pawar et al. [44] suggested that polysaccharides with good micromeritic properties can be used in the formulation of tablets prepared by direct compression.

3.3. Viscosity. Figure 2(e) shows that an increase in the amount of the sample increased the intrinsic viscosity. The highest value of η_{int} was 1.983 ± 0.01 dL/g at 0.8% (w/v), and the lowest value was 0.121 ± 0.02 dL/g at 0.1% (w/v). Intrinsic viscosity reflects the hydrodynamic volume occupied by an individual polymer molecule. Previous studies reported intrinsic viscosity values from 0.8 to 5.48 dL/g [45].

3.4. Total Phenolic Content. The TPC was calculated using the linear regression equation determined ($Y = 1.4378X + 0.0413$, $R^2 = 0.9966$). Our result (5.722 ± 0.113 mg EAG/g) was lower than 67.66 ± 4.71 mg EAG/g [8]. The lower phenolic content is

probably due to the fact that the germination of the corn kernel (during the elaboration of “chicha de jora”) decreases the phenolic content, in agreement with the investigation of Ramadan et al. [46]. Likewise, Rao and Muralikrishna [47] showed a decrease in the phenolic content of FAX extracted from rice after a malting process. On the other hand, our result is slightly higher than the result previously reported for the polysaccharide (3.29 mg EAG/g) extracted from the corn bran [48], and these authors also conclude that the profile of hydroxycinnamic acids varies according to the extraction conditions and the source of the corn fiber.

3.5. Identification of Monosaccharides by Thin-Layer Chromatography (TLC). Figure 3 shows that the sample presented dark blue stains with similar migration to the standards of D-xylose and L-arabinose. However, the sample showed a tail-shaped stain probably related to the presence of other monosaccharides. The sample did not present a stain related to the D-glucose standard. The R_f and R_G of the sample were similar to the standards of D-xylose and L-arabinose (Table 3). In qualitative terms, the identification of the monosaccharides determined by TLC was similar to that reported in the study by Saghir et al. [49]. Li and Du [50] reported that FAX has a low proportion of galactose.

3.6. Analysis by HPLC-MS/MS. Figure 4(a) presents the chromatogram of the FAX hydrolyzed by acid methanolysis under parallel reaction monitoring of m/z 163.06112 with 5 peaks at R_t of 5.92, 6.62, 7.21, 7.47, and 7.69 min. Each peak has a mass spectrum with different fragmentation patterns, suggesting that the sample releases methylated pentoses with different spatial configuration, but similar molecular weight. Mass spectrometry does not allow discriminating compounds that have the same molecular weight and differ in the spatial arrangement, as is the case of L-arabinose and D-xylose (diastereomers at C-4). Figure 5(a) presents the mass spectrum in ESI (–) for the highest relative abundance peak (R_t, 7.21 min), with a first ion with m/z 163.0616. Mocsai et al. [51] suggest that the methylation of monosaccharides from FAX mainly shows methylation at C-3. The ions of m/z 145.05 and m/z 131.03 could correspond to the neutral loss by fragmentation of H₂O and CH₃OH, respectively, in concordance with spectrum reported by Nagar et al. [52]. Likewise, the fragment with peak m/z 59.01 agrees with the spectrum obtained for arabinopyranose (record PS109408) published in the MassBank mass spectra database (<https://www.massbank.jp>; accessed on 21 December 2021). Therefore, it is suggested that the fragmentation pattern after hydrolyzing FAX would correspond to the presence of molecules of methyl-pentofuranosides or methyl-pentopyranosides (diastereomers).

On the other hand, the chromatographic profile of the hydrolyzed FAX (see Figure 6(a)) determined under parallel reaction monitoring of m/z 193.0506 showed 5 peaks (t_R 8.18, 9.32, 9.99, 10.86, and 11.17 min) with different fragmentation patterns. The spectrum of Figure 5(b) for the peak

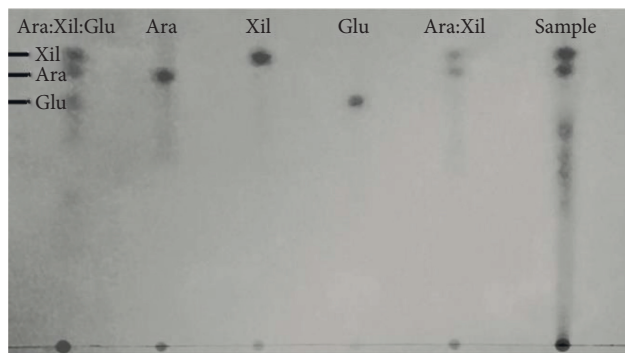


FIGURE 3: Separation of L-arabinose :D-xylose :D-glucose (Ara :Xyl :Glu), L-arabinose (Ara), D-xylose (Xyl), D-glucose (Glu), L-arabinose :D-xylose (Ara: Xil), and the hydrolyzed sample.

TABLE 3: Migration distances, Rf, and RG values of the standards and sample.

Sample seeded	Md (cm)*	Rf**	RG***
L-arabinose :D-xylose :D-glucose	9.4	0.73	1.19
	9.0	0.70	1.14
	8.0	0.63	1.01
L-arabinose	9.0	0.70	1.14
D-xylose	9.4	0.73	1.19
D-glucose	7.9	0.62	1.00
L-arabinose :D-xylose	9.4	0.73	1.19
	8.9	0.69	1.12
Sample (hydrolyzed)	9.4	0.73	1.19
	9.0	0.70	1.14

*Md = migrated distance in cm from seeding origin, **Rf = retention factor; ***RG = retention factor relative to D-glucose.

with the highest relative abundance (Rt, 10.86 min) shows a first ion with m/z 193.0725, and these could be related to the fragmentation profile of ferulic acid; however, according to Sinosaki et al. [53] and He et al. [54], ferulic acid presents three characteristic m/z : m/z 193 (related to the deprotonation of the carboxylic acid), m/z 178 (corresponding to the loss of the methoxy group), and m/z 134 corresponding to the loss of carbonyl; in this sense, the spectrum obtained could not be related to ferulic acid. The precursor ions with m/z , 193.07304; m/z , 193.07368; m/z , 193.07314; m/z , 193.07274; and m/z , 193.07285 (Figures 6(b)–6(f)) contain fragments that could correspond possibly to methyl-hexafuranosides or methyl-hexapyranosides (diastereomers). This after comparing with the mass spectrum of a methyl-hexopyranoside (m/z 193.07174, [H-]) was published in the PubChem database (<https://pubchem.ncbi.nlm.nih.gov/>; accessed on 21 December 2021) with four fragments (m/z , 59.013; m/z , 71.013; m/z , 85.029; m/z , 101.023).

3.7. UV-Vis Spectroscopy. The UV-vis spectroscopy was made mainly for the identification of the ferulic acid, considering that the functional groups of the polysaccharides present little or no absorptivity in the UV-vis spectrum (Figure 2(f)). Regarding the peak at 280 nm, Guo et al. [55] indicated that it is related to the existence of proteins, which is consistent with the protein quantification. The arm at 325 nm, according to Li et al. [56], is attributed to phenolic compounds attached to arabinose residues. On the other

hand, bands around 324 nm ($n \rightarrow \pi^*$ transition of C=O and C=C bonds connected to the benzene ring) suggests the presence of units of conjugated phenolic compounds (ferulic acid and p-coumaric acid) [57].

3.8. Infrared Spectroscopy. The infrared spectrum (Figure 7) shows characteristic absorption patterns and bands previously identified for FAX by Aslam Khan et al. [58] and Mo et al. [59]. The broad band at 3320 cm^{-1} is attributed to the stretching vibration of the hydroxyl functional group (-OH) [60]. The band pattern at 2970 cm^{-1} and 2880 cm^{-1} correspond to stretching vibrations of the saturated aliphatic group—CH₂ [61]. Additionally, the absorption at 1380 cm^{-1} is assigned to the symmetric C=O strain, which was previously associated with the presence of uronic acid in the FAX structure [55]. The absorption at 1090 cm^{-1} corresponds to the C-O-C antisymmetric stretching vibration typical of the polysaccharide glycosidic bond, while a central band at 1050 cm^{-1} is assigned to the bending vibration of the C-OH bond [62]. At 880 cm^{-1} , a band was observed indicating the β configuration of the enantiomeric carbon of the pyranose units [54]. Like Li et al. [56] and Mo et al. [59], there was no evidence of absorption at 850 cm^{-1} associated with the α configuration of the furanose monosaccharide of arabinose. Likewise, the band at 616 cm^{-1} could be associated with C=C vibration of the aromatic ring of ferulic acid [63]. On the other hand, the IR spectrum obtained did not reflect the existence of proteins, which differs from the research carried out by De Anda-Flores et al. [64], in which the

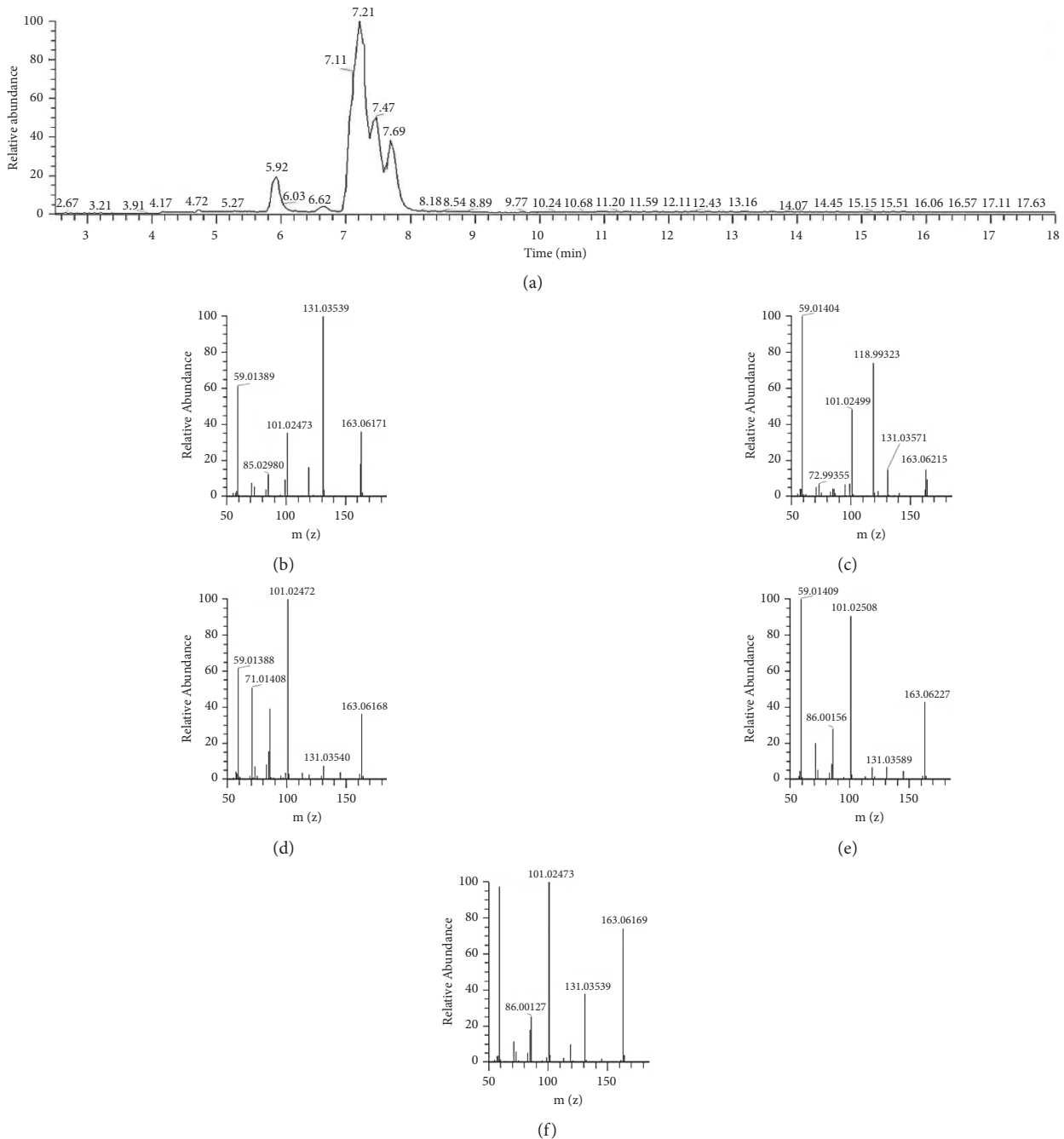


FIGURE 4: (a) Chromatographic profile (LC-MS) of hydrolyzed FAX between Rt of 2.5 and 18.0 min; (b) mass spectrum at Rt 5.92 min; (c) mass spectrum at Rt 6.62 min; (d) mass spectrum at Rt 7.21 min; (e) mass spectrum at Rt 7.47 min; (f) mass spectrum at Rt 7.69 min.

existence of proteins is suggested by showing absorption bands between 1640 and 1533 cm^{-1} .

3.9. Determination of Antioxidant Capacity In Vitro

3.9.1. DPPH• Assay. According to Table 4, FAX showed capacity to inhibit the DPPH• radical (between 0.5 and 10 mg/mL), which increased with the concentration. At 0.5 mg/mL , the inhibition % of the sample was lower ($18.92 \pm 0.84\%$), increasing until $61.66 \pm 0.41\%$ at 10 mg/mL .

At 5 mg/mL , the inhibition% for the sample was $45.25 \pm 0.74\%$, a value slightly higher than 42.64% for FAX from the corn bran [65]. The standard had a lower IC₅₀ value (0.0128 mg/mL), which showed that Trolox has can inhibit the radical approximately 515 times higher than the sample (IC₅₀, 6.5921 mg/mL). The IC₅₀ value obtained was lower than the IC₅₀ (1.3 mg/mL) previously reported for FAX from the rice bran [66]. Within the chemical structure of ferulic acid, the presence of the carbonyl group ($-\text{CO}-$) in the paraposition of the phenolic

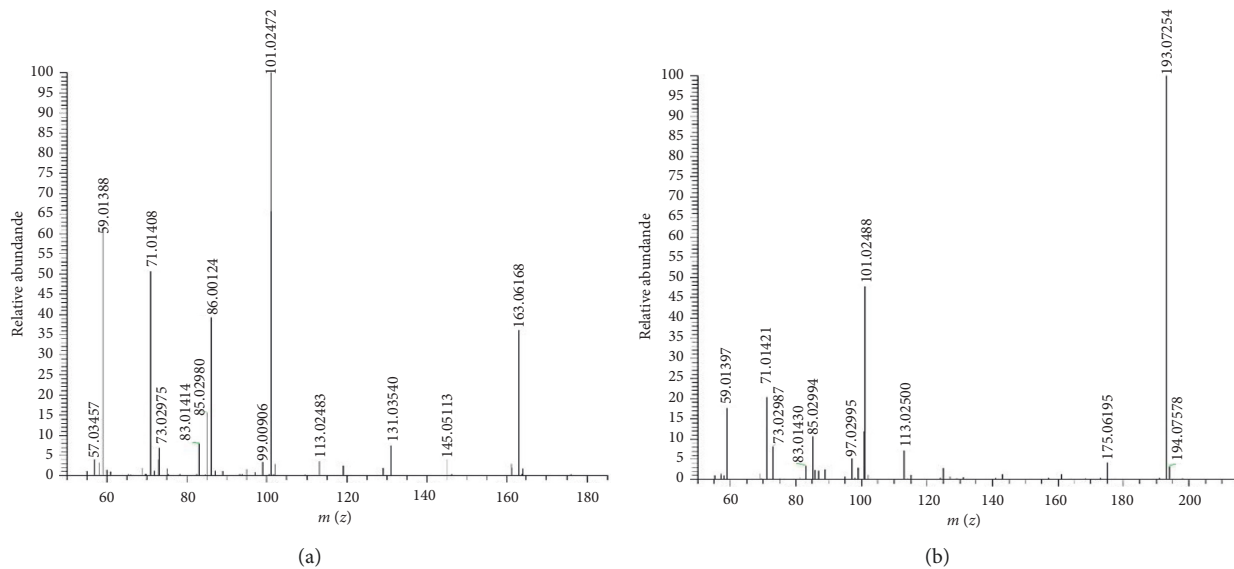


FIGURE 5: (a) Fragmentation of the molecular ion with m/z 163.0611967 $[M-H]^-$ for the main peak at $R_t = 7.21$ min; (b) fragmentation of the molecular ion with m/z 193.0506321 $[M-H]^-$ for the main peak at $R_t = 10.86$ min.

ring causes the delocalization of electrons to give rise to the phenoxy radical [67] which gives the capacity to inhibit the radicals [68]. The Trolox equivalent antioxidant capacity (TEAC) of FAX was $7.7844 \pm 0.08 \mu\text{mol TEAC/g}$ (Table 3) lower than $18 \mu\text{mol TEAC/g}$ for FAX from corn residues derived from industrial ethanol production [23].

3.9.2. ABTS $\bullet+$ Assay. The greatest inhibition of ABTS $\bullet+$ ($71.17 \pm 1.08\%$) occurred at 10 mg/mL; likewise, the lowest inhibition ($0.90 \pm 0.30\%$) was at 0.1 mg/mL (Table 4). Trolox presented an inhibition capacity of approximately 11 times greater than the sample after comparing their IC₅₀ values. Our results are in agreement with the findings of El-Gizawy and Hussein [68], in which FAX presented higher antioxidant capacity in the ABTS $\bullet+$ assay (aqueous medium) compared to the DPPH \bullet assay (partially aqueous medium). FAX shows a hydrophilic behavior, so its antioxidant profile is favored in a medium of the same nature, which generates an increase in the effective concentration of ferulic acid in the aqueous medium [69]. Recently, Marquez-Escalante et al. [70] have reported that FAX from corn distiller's grains derived from industrial alcohol manufacture has an antioxidant capacity of $11.3 \mu\text{mol TEAC/g}$ in the ABTS $\bullet+$ assay. On the other hand, our result is close to the value previously reported by Paz-Samaniego et al. [71] of $39.2 \pm 1 \mu\text{mol TEAC/g}$.

3.9.3. FRAP Assay. The FRAP assay measures the potential of an antioxidant to reduce the ferric ion (Fe^{3+}) to produce the blue-colored ferrous ion (Fe^{2+}) in a low pH medium [72]. In Table 4, the FRAP value of the sample was $36.6 \pm 0.3 \mu\text{mol Fe}^{2+}/\text{g}$, which is higher than the value ($5.6 \mu\text{mol Fe}^{2+}/\text{g}$) previously reported by Hu et al. [73] for commercial FAX. A slightly higher FRAP value ($49 \mu\text{mol Fe}^{2+}/\text{g}$) was obtained for FAX from the residual malted barley grains derived from

beer production [74]. However, our result was lower than $786.2 \mu\text{mol Fe}^{2+}/\text{g}$ [75].

3.10. Determination of In Vitro Antihyperglycemic Capacity

3.10.1. Glucose Adsorption Capacity (GAC). Figure 8 shows that the sample can adsorb 1.81 ± 0.21 , 2.82 ± 0.25 , 6.21 ± 1.23 , and $8.10 \pm 1.63 \text{ mmol/g}$ of glucose. A greater amount of glucose in the medium shows greater amounts of glucose bound to the polysaccharide. The results are indicative that FAX can effectively adsorb glucose, and thus, it could play an important role in lowering postprandial glucose concentrations. The CAG of the sample was greater than the reported value for the insoluble dietary fiber polysaccharide of the rice bran ($0.01\text{--}1.04 \text{ mmol/g}$) [75] and slightly lower than the insoluble dietary fiber polysaccharide of the foxtail "*Setaria italica*" bran ($3.72\text{--}16.74 \text{ mmol/g}$) [26]. The CAG is related to the molecular weight of the polysaccharide [76].

3.10.2. Glucose Diffusion Inhibition Capacity. The glucose diffusion inhibition assay is useful for predicting the effect of a polysaccharide in order to delay the glucose absorption in the gastrointestinal tract [27]. Figure 9 shows that, within each treatment group (negative control, acarbose, FAX 1 mg/mL, FAX 10 mg/mL, and FAX 25 mg/mL), a statistically significant difference ($p < 0.05$) was observed. The increase in the concentration of glucose in the external medium increased rapidly up to 60 min in concordance with the results previously reported for FAX extracted from triticale [77] and for the polysaccharide extracted from *Tuber aestivum* [78]. A comparison with the negative control group allowed us to observe that FAX 10 mg/mL at 30 min and FAX 25 mg/mL (except at 180 min) show a statistically significant difference

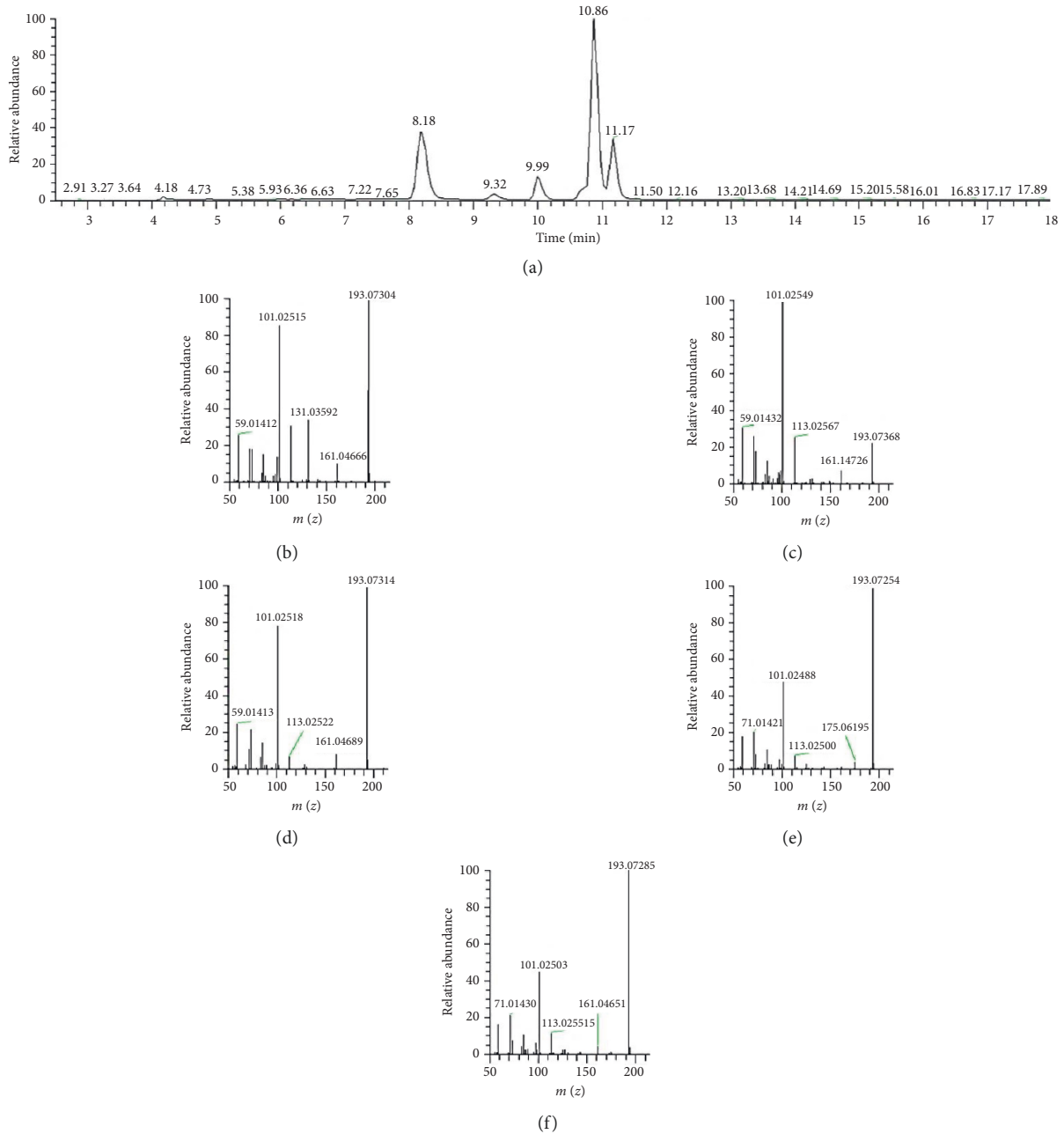


FIGURE 6: (a) Chromatographic profile (LC-MS) of hydrolyzed FAX between Rt of 2.5 and 18.0 min; (b) mass spectrum at Rt 8.18 min; (c) mass spectrum at Rt 9.32 min; (d) mass spectrum at Rt 9.99 min; (e) mass spectrum at Rt 10.86 min; (f) mass spectrum at Rt 11.17 min.

($p < 0.05$), and the other groups inhibited glucose diffusion, but no significant difference was found ($p > 0.05$). Only FAX 25 mg/mL at 90 min showed a statistically significant difference compared with the acarbose. These results may be related to the high viscosity, in which the polysaccharide develops a barrier on the dialysis tube, which reduces the diffusion of glucose. The ability to inhibit glucose diffusion of the polysaccharides may be due to factors such as degree of viscosity, adsorption capacity, formation of physical obstacles, and the ability to trap glucose within a network [79].

3.10.3. α -Amylase Inhibition Capacity. Inhibition of the enzymatic activity of α -amylase may contribute to delaying the increase in postprandial blood glucose levels by decreasing glucose release and delaying its absorption [80]. Among the seven different concentrations (Figure 10), the highest inhibition ($46.6 \pm 0.42\%$) occurred at 5 mg/mL of sample; however, at the same concentration acarbose reached an inhibition of $88.7 \pm 0.33\%$. When the concentration of FAX was 0.1 mg/mL, the inhibition was lower ($11.51 \pm 0.88\%$) compared to acarbose ($46.24 \pm 2.24\%$), at the same concentration. The IC_{50} value of the sample (4.73 ± 0.05 mg/mL) was in agreement with the value

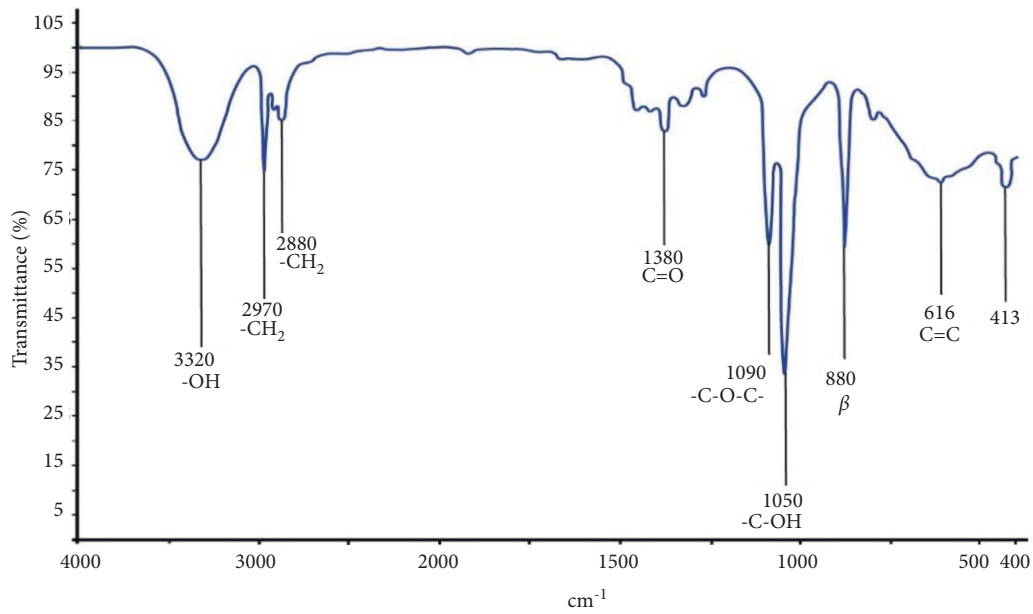
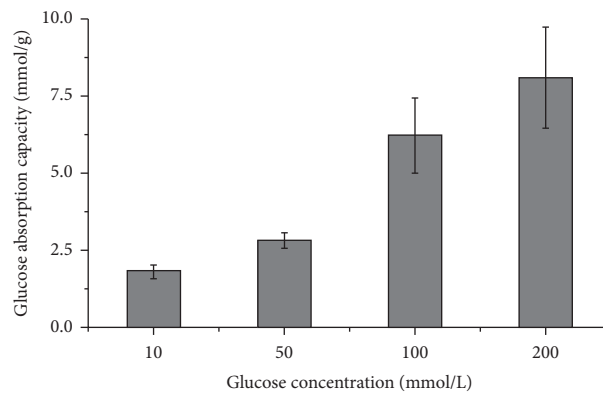


FIGURE 7: Infrared spectrum of the extracted FAX.

TABLE 4: Antioxidant capacity of the extracted AXF determined by the DPPH•, ABTS•+, and FRAP assays.

Sample	In vitro assay					
	DPPH•		ABTS•+		FRAP	
	IC50 (mg/mL)	TEAC ($\mu\text{mol/g}$)	IC50 (mg/mL)	TEAC ($\mu\text{mol/g}$)	FRAP value ($\mu\text{mol AA/g}$)	FRAP value ($\mu\text{mol Fe}^{+2}/\text{g}$)
FAX	$6.59 \pm 0.03^*$	$7.7844 \pm 0.08^*$	$6.50 \pm 0.08^*$	$35.347 \pm 0.94^*$	$14.081 \pm 0.11^*$	$36.63 \pm 0.29^*$
Trolox	$0.013 \pm 0.0001^*$	—	$0.059 \pm 0.0001^*$	—	—	—

*All the results are expressed as the mean \pm S.D. ($n = 3$).

FIGURE 8: Glucose adsorption capacity of FAX in solutions of different concentrations of anhydrous glucose. The results are expressed as the mean \pm S.D. ($n = 3$).

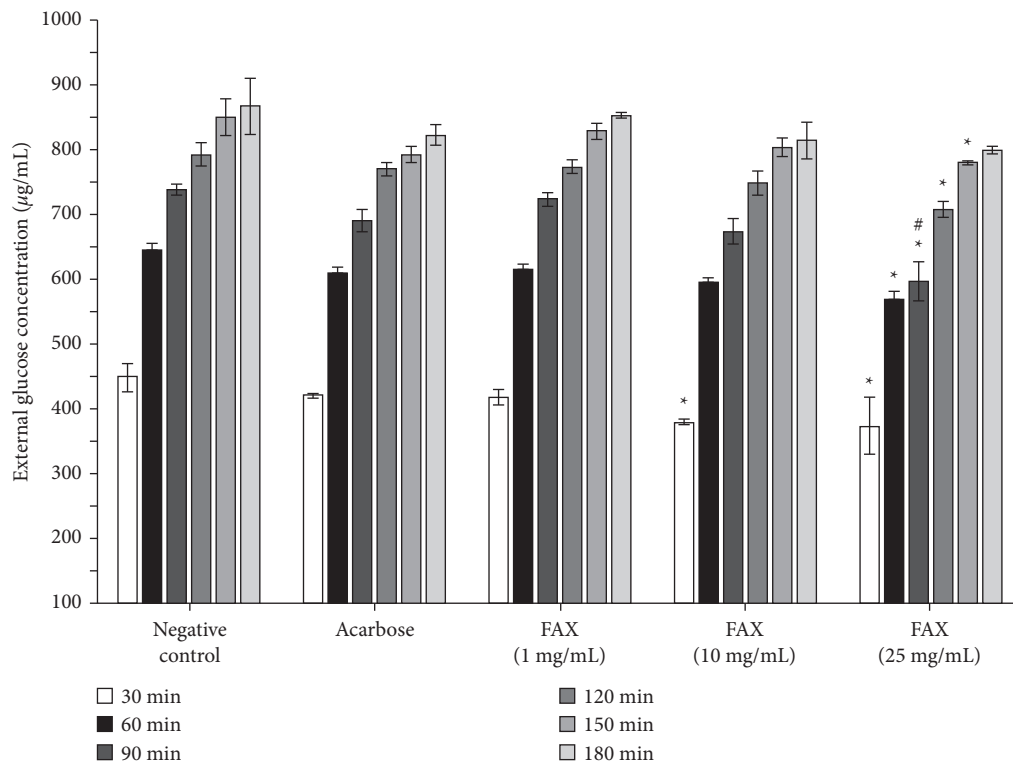


FIGURE 9: Glucose diffusion inhibition capacity of different concentrations of FAX, negative control, and positive control evaluated at different times. The results are expressed as the mean \pm S.D. ($n = 3$). * $p < 0.05$, compared with the negative control. # $p < 0.05$, compared with the acarbose.

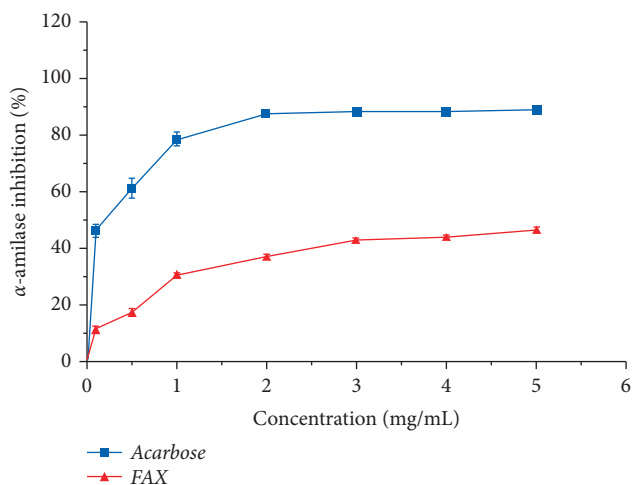


FIGURE 10: FAX and acarbose α -amylase inhibition. The results are expressed as the mean \pm S.D. ($n = 3$).

(IC₅₀ = 5 mg/mL) previously reported for the polysaccharide of the wheat bran [81]. Polysaccharides can limit the rate of digestion of starch by the enzyme α -amylase in two ways [82]. First of all, polysaccharides can form a barrier that decreases or prevents the interaction of the digestive enzyme with starch. Secondly, the chemical nature of the polysaccharides may be related to the inhibition of α -amylase. It has been shown that a high presence of free carboxylic groups, hydroxyl, and methoxy group inhibits the enzymatic hydrolysis of starch [83]. The FAX presents a competitive type

inhibition [76]. It should be noted that it is necessary to develop *in vivo* studies to evaluate the antihyperglycemic capacity of FAX.

4. Conclusions

In the present study, the extraction of FAX from the bagasse of “chicha de jora” was achieved by the alkaline hydrogen peroxide method, the dialyzed polysaccharide with molecular weight ≥ 3.5 kDa had an extraction yield of $19.87 \pm 4.56\%$. The physicochemical analysis allowed corroborating the physicochemical characteristics of the FAX obtained, while the spectrophotometric analysis confirmed the presence of the typical structure of the polysaccharide. The sample shows *in vitro* antioxidant and antihyperglycemic capacity.

Data Availability

The data used to support the findings of this study are included within the article.

Conflicts of Interest

The authors declare no conflicts of interest.

Authors' Contributions

J. J. S.-H. and L. S. V.-S. conceptualized the study; C. M. F.-R. was responsible for methodology; O. H.-C. and C. M. F.-R. validated the study; J. J. S.-H., E. L.-G., E. J. M.-M., J. F. K.-C.,

and J. S. A.-L. contributed to formal analysis; J. J. S.-H. and L. S. V.-S. investigated the study; M. M. A. provided resources; J. J. S.-H. and L. S. V.-S. prepared the original draft; O. H.-C. reviewed and edited the manuscript; O. H.-C. and J. B. P.-O. visualized the study; J. S. A.-G. supervised the study; J. J. S. H. and M. M. A. were responsible for project administration; S. M. acquired funding. All authors have read and agreed to the published version of the manuscript.

Acknowledgments

The authors thank the Universidad Nacional Mayor de San Marcos and the Faculty of Pharmacy and Biochemistry for giving the facilities to carry out this work.

References

- [1] D. Bassi, L. Orrù, J. Cabanillas Vasquez, P. S. Cocconcelli, and C. Fontana, "Peruvian chicha: a focus on the microbial populations of this ancient maize-based fermented beverage," *Microorganisms*, vol. 8, no. 1, pp. 93–13, 2020.
- [2] T. Yoshida, M. Sakamoto, and J. Azuma, "Extraction of hemicelluloses from corn pericarp by the NaOH-urea solvent system," *Procedia Chemistry*, vol. 4, no. 1, pp. 294–300, 2012.
- [3] N. K. Ganguli and M. A. Turner, "A simplified method for extracting water-extractable arabinoxylans from wheat flour," *Journal of the Science of Food and Agriculture*, vol. 88, no. 11, pp. 1905–1910, 2008.
- [4] A. Fadel, A. M. Mahmoud, J. J. Ashworth, W. Li, Y. L. Ng, and A. Plunkett, "Health-related effects and improving extractability of cereal arabinoxylans," *International Journal of Biological Macromolecules*, vol. 109, pp. 819–831, 2018.
- [5] X. Si, Z. Zhou, D. Bu, J. Li, P. Strappe, and C. Blanchard, "Efecto de la sulfatación en las propiedades antioxidantes y las características proliferativas celulares in vitro de polisacáridos aislados de salvado de maíz," *CYTA—Journal of Food*, vol. 14, no. 4, pp. 555–564, 2016.
- [6] D. C. Bernhardt, N. M. A. Ponce, M. F. Basanta, C. A. Stortz, and A. M. Rojas, "Husks of Zea mays as a potential source of biopolymers for food additives and materials' development," *Heliyon*, vol. 5, no. 3, pp. 1–28, 2019.
- [7] J. Li, W. Shang, X. Si et al., "Carboxymethylation of corn bran polysaccharide and its bioactive property," *International Journal of Food Science & Technology*, vol. 52, no. 5, pp. 1176–1184, 2017.
- [8] S. Kamboj and V. Rana, "Physicochemical, rheological and antioxidant potential of corn fiber gum," *Food Hydrocolloids*, vol. 39, no. 1, pp. 1–9, 2014.
- [9] L. N. Malunga, P. Eck, and T. Beta, "Inhibition of intestinal α -glucosidase and glucose absorption by feruloylated arabinoxylan mono and oligosaccharides from corn bran and wheat aleurone," *Journal of Nutrition and Metabolism*, vol. 2016, no. 1, 9 pages, Article ID 1932532, 2016.
- [10] J. Huang, X. Wang, G. Tao et al., "Feruloylated oligosaccharides from maize bran alleviate the symptoms of diabetes in streptozotocin-induced type 2 diabetic rats," *Food & Function*, vol. 9, no. 3, pp. 1779–1789, 2018.
- [11] Q. Nie, M. Xing, H. Chen, J. Hu, and S. Nie, "Metabolomics and lipidomics profiling reveals hypocholesterolemic and hypolipidemic effects of arabinoxylan on type 2 diabetic rats," *Journal of Agricultural and Food Chemistry*, vol. 67, no. 38, pp. 10614–10623, 2019.
- [12] Y. Liu, S. Qiu, J. Li et al., "Peroxidase-mediated conjugation of corn fiber gum and bovine serum albumin to improve emulsifying properties," *Carbohydrate Polymers*, vol. 118, no. 1, pp. 70–78, 2015.
- [13] Z. Zhang, C. Smith, W. Li, and J. Ashworth, "Characterization of nitric oxide modulatory activities of alkaline-extracted and enzymatic-modified arabinoxylans from corn bran in cultured human monocytes," *Journal of Agricultural and Food Chemistry*, vol. 64, no. 43, pp. 8128–8137, 2016.
- [14] C of Europe, *European Pharmacopoeia*, European Directorate for the Quality of Medicines and HealthCare, Strasbourg, France, 2021.
- [15] L. Kong, L. Yu, T. Feng, X. Yin, T. Liu, and L. Dong, "Physicochemical characterization of the polysaccharide from *Bletilla striata*: effect of drying method," *Carbohydrate Polymers*, vol. 125, no. 1, pp. 1–8, 2015.
- [16] Association of Official Analytical Chemists, *Official Methods of Analysis of AOAC International*, Association of Official Analytical Chemists, Gaithersburg, MD, USA, 2000.
- [17] D. Suvakanta, M. P. Narsimha, D. Pulak, C. Joshabir, and D. Biswajit, "Optimization and characterization of purified polysaccharide from *Musa sapientum* L. as a pharmaceutical excipient," *Food Chemistry*, vol. 149, no. 1, pp. 76–83, 2014.
- [18] USPCC, *United States Pharmacopeial*, USPCC, Erlanger, KY, USA, 2013.
- [19] H. Ijaz, U. R. Tulain, F. Azam, and J. Qureshi, "Thiolation of arabinoxylan and its application in the fabrication of pH-sensitive thiolated arabinoxylan grafted acrylic acid copolymer," *Drug Development and Industrial Pharmacy*, vol. 45, no. 5, pp. 754–766, 2019.
- [20] M. A. Kaleem, M. Z. Alam, M. Khan, S. H. Jaffery, and B. Rashid, "An experimental investigation on accuracy of Hausner ratio and Carr index of powders in additive manufacturing processes," *Metal Powder Report*, vol. 30, no. 20, 2020.
- [21] V. Van Craeyveld, *Production and Functional Characterisation of Arabinoxylan-Oligosaccharides from Wheat (Triticum aestivum L.) Bran and Psyllium (Plantago Ovata Forsk) Seed Husk*, University KU Leuven, Leuven, Belgium, 2009.
- [22] A. Eugene, C. Lapierre, and J. Ralph, "Improved analysis of arabinoxylan-bound hydroxycinnamate conjugates in grass cell walls," *Biotechnology for Biofuels*, vol. 13, no. 1, pp. 202–207, 2020.
- [23] J. A. Marquez-Escalante and E. Carvajal-Millan, "Feruloylated arabinoxylans from maize Distiller's dried grains with solubles: effect of feruloyl esterase on their macromolecular characteristics, gelling, and antioxidant properties," *Sustainability*, vol. 11, no. 22, pp. 1–12, 2019.
- [24] L. N. Malunga and T. Beta, "Antioxidant capacity of water-extractable arabinoxylan from commercial barley, wheat, and wheat fractions," *Cereal Chemistry Journal*, vol. 92, no. 1, pp. 29–36, 2015.
- [25] W. Xu, F. Zhang, Y. Luo, L. Ma, X. Kou, and K. Huang, "Antioxidant activity of a water-soluble polysaccharide purified from *Pteridium aquilinum*," *Carbohydrate Research*, vol. 344, no. 2, pp. 217–222, 2009.
- [26] J. I. Dong, L. Wang, J. Lü, Y. Y. Zhu, and R. L. Shen, "Structural, antioxidant and adsorption properties of dietary fiber from foxtail millet (*Setaria italica*) bran," *Journal of the Science of Food and Agriculture*, vol. 99, no. 8, pp. 3886–3894, 2019.
- [27] S. A. Maktoof, I. M. N. Alrubayae, and N. A. Almansorii, "Evaluation of in vitro antidiabetic effect and phytochemical screening of some wild mushroom extracts isolated in Basrah,

- Iraq," *Drug Invention Today*, vol. 11, no. 11, pp. 2797–2803, 2019.
- [28] M. A. Inocente Camones, B. Jurado-Teixeira, B. Jurado Teixeira et al., "Actividad hipoglucemiante in vitro de los polisacáridos digeridos de *Nostoc sphaericum* Vaucher ex Bornet & Flahault (cushuro)," *Horizonte Médico (Lima)*, vol. 19, no. 1, pp. 26–31, 2019.
- [29] M. P. Yadav, D. B. Johnston, A. T. Hotchkiss, and K. B. Hicks, "Corn fiber gum: a potential gum Arabic replacer for beverage flavor emulsification," *Food Hydrocolloids*, vol. 21, no. 7, pp. 1022–1030, 2007.
- [30] K. Buksa, W. Praznik, R. Loeppert, and A. Nowotna, "Characterization of water and alkali extractable arabinoxylan from wheat and rye under standardized conditions," *Journal of Food Science and Technology*, vol. 53, no. 3, pp. 1389–1398, 2016.
- [31] S. E. Broxterman, *The Architecture of the Primary Plant Cell Wall: The Role of Pectin Reconsidered*, Wageningen University, Wageningen, Netherlands, 2018.
- [32] C. Maes and J. A. Delcour, "Alkaline hydrogen peroxide extraction of wheat bran non-starch polysaccharides," *Journal of Cereal Science*, vol. 34, no. 1, pp. 29–35, 2001.
- [33] A. Höjje, M. Gröndahl, K. Tømmersaas, and P. Gatenholm, "Isolation and characterization of physicochemical and material properties of arabinoxylans from barley husks," *Carbohydrate Polymers*, vol. 61, no. 3, pp. 266–275, 2005.
- [34] S. Naz, N. Ahmad, J. Akhtar, N. M. Ahmad, A. Ali, and M. Zia, "Management of citrus waste by switching in the production of nanocellulose," *IET Nanobiotechnology*, vol. 10, no. 6, pp. 395–399, 2016.
- [35] B. Lindman, G. Karlström, and L. Stigsson, "On the mechanism of dissolution of cellulose," *Journal of Molecular Liquids*, vol. 156, no. 1, pp. 76–81, 2010.
- [36] R. M. Bell, *Extraction of Arabinoxylan from Animal Feed and Investigations into its Functionality as an Ingredient in Bread Dough*, University of Manchester, Manchester, UK, 2015.
- [37] F. Leong, X. Hua, M. Wang et al., "Quality standard of traditional Chinese medicines: comparison between European pharmacopoeia and Chinese pharmacopoeia and recent advances," *Chinese Medicine*, vol. 15, no. 1, pp. 76–20, 2020.
- [38] M. G. Ji, Y. R. Lee, Y. H. Nam, R. Castañeda, B. N. Hong, and T. H. Kang, "Immunostimulatory action of high-content active arabinoxylan in rice bran," *ACS Omega*, vol. 5, no. 1, pp. 26374–26381, 2020.
- [39] L. Yang, J. Cao, Y. Jin et al., "Effects of sodium carbonate pretreatment on the chemical compositions and enzymatic saccharification of rice straw," *Bioresource Technology*, vol. 124, no. 1, pp. 283–291, 2012.
- [40] L. Jacquemin, R. Zeitoun, C. Sablayrolles, P.-Y. Pontalier, and L. Rigal, "Evaluation of the technical and environmental performances of extraction and purification processes of arabinoxylans from wheat straw and bran," *Process Biochemistry*, vol. 47, no. 3, pp. 373–380, 2012.
- [41] R. González-Estrada and E. Carvajal-Millan, "Covalently cross-linked arabinoxylans films for debaryomycetans entrapment," *Molecules*, vol. 20, no. 1, pp. 11373–11386, 2015.
- [42] M. A. Mendez-Encinas, E. Carvajal-Millan, A. Rascon-Chu, H. F. Astiazaran-Garcia, and D. E. Valencia-Rivera, "Ferulated arabinoxylans and their gels: functional properties and potential application as antioxidant and anticancer agent," *Oxidative Medicine and Cellular Longevity*, vol. 2018, no. 1, pp. 1–22, 2018.
- [43] A. Erum, S. Bashir, and S. Saghir, "Modified and unmodified arabinoxylans from *Plantago ovata* husk: novel excipients with antimicrobial potential," *Journal of Pharmacology*, vol. 10, no. 1, pp. 765–769, 2015.
- [44] H. A. Pawar, A. J. Gavasane, and P. D. Choudhary, "Extraction of polysaccharide from fruits of *Cordia dichotoma* G. Forst using acid precipitation method and its physicochemical characterization," *Biological Macromolecules*, vol. 9554, no. 1, pp. 1–21, 2018.
- [45] A. Shah, F. A. Masoodi, A. Gani et al., *Food Biopolymers: Structural, Functional and Nutraceutical Properties*, Springer Nature Switzerland, Berlin, Germany, 2021.
- [46] B. R. Ramadan, M. A. Sorour, and M. A. Kelany, "Changes in total phenolics and DPPH scavenging activity during domestic processing in some cereal grains," *Annals Food Science and Technology*, vol. 13, no. 2, pp. 190–196, 2012.
- [47] R. S. P. Rao and G. Muralikrishna, "Water soluble feruloyl arabinoxylans from rice and ragi: changes upon malting and their consequence on antioxidant activity," *Phytochemistry*, vol. 67, no. 1, pp. 91–99, 2006.
- [48] F. E. Ayala-Soto, S. O. Serna-Saldívar, S. García-Lara, and E. Pérez-Carrillo, "Hydroxycinnamic acids, sugar composition and antioxidant capacity of arabinoxylans extracted from different maize fiber sources," *Food Hydrocolloids*, vol. 35, no. 1, pp. 471–475, 2014.
- [49] S. Saghir, M. Saeed, M. Ajaz, A. Koschella, and T. Heinze, "Structure characterization and carboxymethylation of arabinoxylan isolated from *Ispaghula* (*Plantago ovata*) seed husk," *Carbohydrate Polymers*, vol. 74, no. 1, pp. 309–317, 2008.
- [50] J. Li and J. Du, "Molecular characterization of arabinoxylan from wheat beer," *Molecules*, vol. 24, pp. 1–15, 2019.
- [51] R. Mócsai, R. Figl, L. Sützl, S. Fluch, and F. Altmann, "A first view on the unsuspected intragenus diversity of N-glycans in *Chlorella* microalgae," *The Plant Journal: For Cell and Molecular Biology*, vol. 103, no. 1, pp. 184–196, 2020.
- [52] S. Nagar, A. Hensel, P. Mischnick, and V. Kumar, "A unique polysaccharide containing 3-O-methylarabinose and 3-O-methylgalactose from *Tinospora sinensis*," *Carbohydrate Polymers*, vol. 193, no. 13432, pp. 326–335, 2018.
- [53] N. B. M. Sinosaki, A. P. P. Tonin, M. A. S. Ribeiro et al., "Structural study of phenolic acids by triple quadrupole mass spectrometry with electrospray ionization in negative mode and H/D isotopic exchange," *Journal of Brazilian Chemical Society*, vol. 31, no. 2, pp. 402–408, 2020.
- [54] M. He, G. Peng, F. Xie, L. Hong, and Q. Cao, "Liquid chromatography-high-resolution mass spectrometry with ROI strategy for non-targeted analysis of the in vivo/in vitro ingredients coming from *ligusticum chuanxiong* hort," *Chromatographia*, vol. 82, no. 7, pp. 1069–1077, 2019.
- [55] R. Guo, Z. Xu, S. Wu et al., "Molecular properties and structural characterization of an alkaline extractable arabinoxylan from hull-less barley bran," *Carbohydrate Polymers*, vol. 218, no. 2, pp. 250–260, 2019.
- [56] Y. Li, T. He, R. Liang, Z. Luo, Y. Zhu, and C. Yang, "Preparation and properties of multifunctional sinapic acid corn bran arabinoxylan," *International Journal of Biological Macromolecules*, vol. 8130, no. 1, pp. 1279–1287, 2017.
- [57] D. Xie, T. Gan, C. Su, Y. Han, Z. Liu, and Y. Cao, "Structural characterization and antioxidant activity of water-soluble lignin-carbohydrate complexes (LCCs) isolated from wheat straw," *International Journal of Biological Macromolecules*, vol. 161, no. 1, pp. 315–324, 2020.
- [58] M. U. Aslam Khan, A. Haider, S. I. Abd Razak et al., "Arabinoxylan/graphene-oxide/nHAP-NPs/PVA bionano composite scaffolds for fractured bone healing," *Journal of Tissue*

- Engineering and Regenerative Medicine*, vol. 15, no. 4, pp. 322–335, 2021.
- [59] Q. Mo, L. Dai, J. Ma, X. Zhao, and L. Zhu, “Preparation and physiological activities of carboxymethylated derivative purified from corn bran,” *IOP Conference Series: Materials Science and Engineering*, vol. 207, no. 1, pp. 1–7, 2017.
- [60] L. M. Flórez-Pardo, A. González-Córdoba, and J. E. López-Galán, “Characterization of hemicelluloses from leaves and tops of the CC 8475, CC 8592, and V 7151 varieties of sugarcane (*Saccharum officinarum* L.),” *Revista DYNA*, vol. 86, no. 210, pp. 98–107, 2019.
- [61] N. Velkova, A. Doliška, L. Fras Zemljič, A. Vesel, B. Saake, and S. Strnad, “Influence of carboxymethylation on the surface physical-chemical properties of glucuronoxylan and arabinoxylan films,” *Polymer Engineering and Science*, vol. 55, no. 12, pp. 2706–2713, 2015.
- [62] H. Yang, R. Yan, H. Chen, D. H. Lee, and C. Zheng, “Characteristics of hemicellulose, cellulose and lignin pyrolysis,” *Fuel*, vol. 86, no. 12–13, pp. 1781–1788, 2007.
- [63] A. Aarabi, M. Honarvar, M. Mizani, H. Faghian, and A. Gerami, “Extraction and purification of ferulic acid as an antioxidant from sugar beet pulp by alkaline hydrolysis,” *Italian Journal of Food Science*, vol. 28, no. 3, pp. 362–375, 2016.
- [64] Y. De Anda-Flores, E. Carvajal-Millan, J. Lizardi-Mendoza et al., “Covalently cross-linked nanoparticles based on ferulated arabinoxylans recovered from a distiller’s dried grains byproduct,” *Processes*, vol. 8, no. 6, p. 691, 2020.
- [65] Y. Jiang, X. Bai, S. Lang, Y. Zhao, C. Liu, and L. Yu, “Optimization of ultrasonic-microwave assisted alkali extraction of arabinoxylan from the corn bran using response surface methodology,” *International Journal of Biological Macromolecules*, vol. 128, no. 1, pp. 452–458, 2019.
- [66] P. Yuwang, I. Sulaeva, J. Hell et al., “Phenolic compounds and antioxidant properties of arabinoxylan hydrolysates from defatted rice bran,” *Journal of the Science of Food and Agriculture*, vol. 98, no. 1, pp. 140–146, 2018.
- [67] D. H. Truong, N. T. A. Nhung, and D. Q. Dao, “Iron ions chelation-based antioxidant potential vs. pro-oxidant risk of ferulic acid: a DFT study in aqueous phase,” *Computational and Theoretical Chemistry*, vol. 1185, no. 1, Article ID 112905, 2020.
- [68] H. A.-E. El-Gizawy and M. A. Hussein, “Isolation, structure elucidation of ferulic and coumaric acids from fortunella japonica swingle leaves and their structure antioxidant activity relationship,” *Free Radicals and Antioxidants*, vol. 7, no. 1, pp. 23–30, 2016.
- [69] Z. Chen, S. Li, Y. Fu, C. Li, D. Chen, and H. Chen, “Arabinoxylan structural characteristics, interaction with gut microbiota and potential health functions,” *Journal of Functional Foods*, vol. 54, pp. 536–551, 2019.
- [70] J. A. Marquez-Escalante, A. Rascón-Chu, A. Campa-Mada, K. G. Martínez-Robinson, and E. Carvajal-Millan, “Influence of carboxymethylation on the gelling capacity, rheological properties, and antioxidant activity of feruloylated arabinoxylans from different sources,” *Journal of Applied Polymer Science*, vol. 137, no. 5, pp. 1–10, 2020.
- [71] R. Paz-Samaniego, M. Méndez-Encinas, and J. M. Fierro-Islas, “Ferulated arabinoxylans recovered from low-value maize byproducts: gelation and antioxidant capacity,” *Antioxidant Properties, Uses and Potential Health Benefits*, Nova Science Publishers, vol. 1, no. 1, Hauppauge, NY, USA, 2014.
- [72] R. Apak, K. Güçlü, B. Demirata et al., “Comparative evaluation of various total antioxidant capacity assays applied to phenolic compounds with the CUPRAC assay,” *Molecules*, vol. 12, no. 7, pp. 1496–1547, 2007.
- [73] S. Hu, J. Yin, S. Nie et al., “In vitro evaluation of the antioxidant activities of carbohydrates,” *Bioactive Carbohydrates and Dietary Fibre*, vol. 7, no. 2, pp. 19–27, 2016.
- [74] J. G. Pérez-Flores, E. Contreras-López, A. Castañeda-Ovando et al., “Physicochemical characterization of an arabinoxylan-rich fraction from brewers’ spent grain and its application as a release matrix for caffeine,” *Food Research International*, vol. 116, no. 7, pp. 1020–1030, 2019.
- [75] P. Yuwang, *Chemical and Antioxidant Properties of Arabinoxylan Hydrolysates from Rice Bran*, School of Food Technology Institute of Agricultural Technology Suranaree University of Technology, Nakhon Ratchasima, Thailand, 2017.
- [76] H. Chen, Y. Liu, T. Yang et al., “Interactive effects of molecular weight and degree of substitution on biological activities of arabinoxylan and its hydrolysates from triticale bran,” *International Journal of Biological Macromolecules*, vol. 166, pp. 1409–1418, 2021.
- [77] H. Chen, Z. Chen, Y. Fu et al., “Structure, antioxidant, and hypoglycemic activities of arabinoxylans extracted by multiple methods from triticale,” *Antioxidants*, vol. 8, no. 12, pp. 584–599, 2019.
- [78] D. S. Mudliyar, J. H. Wallenius, D. K. Bedade, R. S. Singhal, N. Madi, and S. S. Shamekh, “Ultrasound assisted extraction of the polysaccharide from tuber aestivum and its in vitro anti-hyperglycemic activity,” *Bioactive Carbohydrates and Dietary Fibre*, vol. 20, no. 8, pp. 100198–100207, 2019.
- [79] Y. Zheng, B. Xu, P. Shi et al., “The influences of acetylation, hydroxypropylation, enzymatic hydrolysis and crosslinking on improved adsorption capacities and in vitro hypoglycemic properties of millet bran dietary fibre,” *Food Chemistry*, vol. 368, no. 8, pp. 130883–130894, 2022.
- [80] E. Azzopardi, C. Lloyd, S. R. Teixeira, R. S. Conlan, and I. S. Whitaker, “Clinical applications of amylase: novel perspectives,” *Surgery*, vol. 160, no. 1, pp. 26–37, 2016.
- [81] L. N. Malunga, M. Izydorczyk, and T. Beta, “Antiglycemic effect of water extractable Arabinoxylan from wheat aleurone and bran,” *Journal of Nutrition and Metabolism*, vol. 2017, no. 3, pp. 1–6, 2017.
- [82] S. Dhital, F. J. Warren, P. J. Butterworth, P. R. Ellis, and M. J. Gidley, “Mechanisms of starch digestion by α -amylase-structural basis for kinetic properties,” *Critical Reviews in Food Science and Nutrition*, vol. 57, no. 5, pp. 875–892, 2017.
- [83] L. Gong, D. Feng, T. Wang, Y. Ren, Y. Liu, and J. Wang, “Inhibitors of α -amylase and α -glucosidase: potential linkage for whole cereal foods on prevention of hyperglycemia,” *Food Science & Nutrition*, vol. 8, no. 12, pp. 6320–6337, 2020.